Modeling and speciation study of uranium (VI) and technetium (VII) co-extraction with DEHiBA

Moeyaert, P.; Dumas, T.; Guillaumont, D.; Kvashnina, K.; Sorel, C.; Miguirditchian, M.; Dufrêche, P. M. J.-F.;

Originally published:

June 2016

Inorganic Chemistry 55(2016)13, 6511-6519

DOI: https://doi.org/10.1021/acs.inorgchem.6b00595

Modeling and speciation study of uranium(VI) and technetium(VII) co-extraction with DEHiBA

Journal:	*Inorganic Chemistry*
Manuscript ID	ic-2016-00595k.R1
Manuscript Type:	Article
Date Submitted by the Author:	17-May-2016
Complete List of Authors:	Moeyaert, Pauline; CEA Marcoule, DRCP Dumas, Thomas; CEA, Marcoule, Nuclear Energy Division, RadioChemistry & Processes Department, DRCP Guillaumont, Dominique; CEA, DRCP Kvashnina, Kristina; European Synchrotron Radiation Facility, Sorel, Christian; CEA Marcoule Miguirditchian, Manuel; CEA Marcoule, DRCP/SCPS/LCSE Moisy, Philippe; CEA, Dufrêche, Jean-Francois; Institut de Chimie Séparative de Marcoule (ICSM) UMR 5257, UMR 5257 CEA-CNRS-Université Montpellier-ENSCM

Modeling and speciation study of uranium(VI) and technetium(VII) co-extraction with DEHiBA

Pauline Moeyaert[a], Thomas Dumas[a], Dominique Guillaumont[a], Kristina Kvashnina[b, c], Christian Sorel[a], Manuel Miguirditchian[a], Philippe Moisy[a] and Jean-François Dufrêche[d]

a French Alternative Energies and Atomic Energy Commission, CEA, Nuclear Energy Division, Radio Chemistry & Processes Department, DRCP, BP 17171, F-30207 Bagnols sur Cèze, France. E-mail: manuel.miguirditchian@cea.fr; Tel: +33 4 66 79 90 09

b European Synchrotron Radiation Facility, 38000 Grenoble, France

c Helmholtz Zentrum Dresden-Rossendorf, Institute of Resource Ecology, 01314 Dresden, Germany

d Institut de Chimie Séparative de Marcoule, Université de Montpellier 2, UMR 5257 CEA / CNRS / UM2 / ENSCM BP 17171 30207 Bagnols sur Cèze Cedex, France.

KEYWORDS - *N,N*-dialkylamides, DEHiBA, technetium, uranium, solvent extraction, modeling, speciation

ABSTRACT - The *N,N*-dialkylamide DEHiBA (*N,N*-di-2-ethylhexyl-isobutyramide) is a promising alternative extractant to TBP (tri-*n*-butylphosphate) to selectively extract uranium(VI) from plutonium(IV) and spent nuclear fuel fission products. Extraction of technetium, present as

pertechnetic acid ($HTcO_4$) in the spent fuel solution, by DEHiBA was studied for different nitric acid and uranium concentrations. The uranium(VI) and technetium(VII) co-extraction mechanism with DEHiBA was investigated to better understand the behavior of technetium in the solvent extraction process. Uranium and technetium distribution ratios were first determined from batch experiments. Based on these data, a thermodynamic model was developed. This model takes into account deviations from ideality in the aqueous phase using the simple solutions concept. A good representation of uranium and technetium distribution data was obtained when considering the formation of $\overline{(\mathrm{DEHiBA})_i(\mathrm{HNO_3})_j(\mathrm{HTcO_4})_k}$ complexes as well as mixed $\overline{(\mathrm{DEHiBA})_2(\mathrm{UO_2})(\mathrm{NO_3})(\mathrm{TcO_4})}$ and $\overline{(\mathrm{DEHiBA})_3(\mathrm{UO_2})(\mathrm{NO_3})(\mathrm{TcO_4})(\mathrm{HNO_3})}$ complexes where one pertechnetate anion replaces one nitrate in the uranium coordination sphere in the two complexes $\overline{(\mathrm{DEHiBA})_2(\mathrm{UO_2})(\mathrm{NO_3})_2}$ and $\overline{(\mathrm{DEHiBA})_3(\mathrm{UO_2})(\mathrm{NO_3})_2(\mathrm{HNO_3})}$. Combination of complementary spectroscopic techniques (FT-IR and X-ray absorption) supported by theoretical calculations (Density Functional Theory) enabled full characterization of the formation of mixed uranium-technetium species $\overline{(\mathrm{DEHiBA})_2(\mathrm{UO_2})(\mathrm{NO_3})(\mathrm{TcO_4})}$ in the organic phase for the first time. The structural parameters of this complex are reported in the paper and lead to the conclusion that the pertechnetate group coordinates the uranyl cation in a monodentate fashion in the inner coordination sphere. This study shows how combining a macroscopic approach (distribution data acquisition and modeling) with molecular-scale investigations (FT-IR and X-ray absorption analysis supported by theoretical calculations) can provide a new insight into the description of a solvent extraction mechanism.

INTRODUCTION

Technetium is one of the major fission products generated by irradiation of nuclear fuel (6.06% produced from thermal neutron fission of ^{235}U). [1] ^{99}Tc is considered as a long-lived

radioelement (2.1×10^5 yr) [2, 3] and as partially mobile in the geosphere depending on geological conditions. It is therefore an important element to consider when developing processes for managing spent nuclear fuel. During dissolution of irradiated fuel in nitric acid, the first step of the PUREX process [4], technetium is either present as solid metallic particles or oxidized to Tc(VII), its most stable oxidation state in nitric acid solution, to form pertechnetic acid $HTcO_4$. This strong acid easily dissociates to form the oxo-anion TcO_4^- that may interfere with uranium, plutonium and zirconium in the extraction cycles of the PUREX process. [5-7] Indeed, technetium(VII) is mainly co-extracted with uranium(VI) by substituting one nitrate in the uranium-TBP complex [6, 8] but can be efficiently separated from uranium by a dedicated scrubbing step at high acidity in the process. Though technetium is currently collected with the other fission products and conditioned as glass matrix in the reprocessing plants, it has been shown that an adaptation of the PUREX flowsheet is possible to isolate and quantitatively recover Tc for a specific conditioning purpose. [4]

In the framework of the development of Generation IV reactors, new liquid-liquid extraction processes for the recycling of future spent nuclear fuel are being studied. Monoamides (or *N,N*-dialkylamides) are considered as alternatives to the neutral extractant TBP due to their ability to extract uranium from nitric acid, their high selectivity for uranium(VI) versus plutonium(IV) and fission products (for some branched alkyl *N,N*-dialkylamides), their complete incinerability and the nature of their radiolysis and hydrolysis products. [9-12] New investigations have been recently undertaken with *N,N*-di-2-ethylhexyl-isobutyramide (DEHiBA, **Figure 1**) to develop an innovative solvent extraction process devoted to selective recovery of uranium. [13] These studies confirmed the high potential of the DEHiBA extracting molecule for selective extraction of uranium but also showed a partial extraction of technetium with DEHiBA. In the PUREX

process, it is necessary to study and understand the extraction mechanism of Tc(VII) to the organic phase to correctly model the extraction equilibria and simulate the behavior of this element in the solvent extraction process.

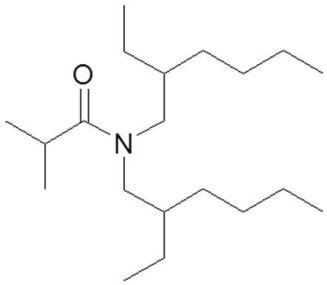

Figure 1. Scheme of *N,N*-di-2-ethylhexyl-isobutyramide (DEHiBA)

Thermodynamic modeling can be used to gain more information on the extraction equilibria of Tc(VII) by DEHiBA. Though the matrix of spent nuclear fuel in the reprocessing step is complex and deviates from ideality, a thermodynamic approach based on the simple solutions theory can be used to model the behavior of the electrolytes of interest in spent nuclear fuels. [14, 15] Stoichiometries of the extracted species, which provide crucial information on extraction mechanisms can be determined from the thermodynamic model; however, they do not provide insight into metal inner- or outer sphere coordination and further knowledge of molecular structures of actinide ions in the organic phase is essential for a comprehensive understanding of metal-selective extraction processes.

Spectroscopic measurements of the organic phase can provide some structural information on complexes in the organic phase. Combining the two techniques can give a more detailed picture. For instance, co-extraction of pertechnetate anion in the uranium-TBP complex is well-known from extraction data but very few coordination studies have helped to characterize these species in the organic phase. [16, 17] Thus, the purpose of the present work is to investigate the extraction behavior of technetium by DEHiBA diluted in the industrial diluent TPH (hydrogenated

tetrapropylene, a branched dodecane), and its co-extraction with uranium. Extraction isotherms of technetium with and without uranium were acquired and modeled by taking into account the deviations from ideality. A speciation study based on spectroscopic investigations using Fourier transform infrared and X-ray absorption (EXAFS), supported by density functional theory (DFT) calculations, was then performed to define uranium(VI) and technetium(VII) speciation in the organic phase and to probe the uranium coordination sphere. Finally both macroscopic thermodynamic modeling and microscopic spectroscopic results are discussed.

EXPERIMENTAL

Reagents

DEHiBA was synthesized by Pharmasynthese (INABATA group) and diluted at 1 $mol.L^{-1}$ in TPH (Novasep process). Its purity (> 99%) was checked by Nuclear Magnetic Resonance (NMR) and mass spectrometry (GC-MS). An aqueous stock solution of pertechnetic acid was prepared starting with pure $NH_4{}^{99}TcO_4$ following the procedure described by Boyd and Moeyaert et al [18, 19]. Solutions of 10^{-3} M $HTcO_4$ spiked with ^{99m}Tc (provided by Cis-Bio IBA) were prepared at different nitric acid concentrations from 0.01 to 8 M for technetium solvent extraction experiments. The uranium stock solution used to prepare solutions with nitric acid and technetium was prepared from uranyl nitrate purchased from Prolabo and titrated using X-Ray fluorescence (Quant'X from ThermoFisher Scientific). All other high grade chemical reagents (HNO_3, NaOH, EtOH, …) were purchased from Prolabo and used without further purification.

Methods

Solvent extraction experiments

Solvent extraction experiments were performed in glovebox in the ATALANTE facility by vigorous shaking of equal volumes of organic and aqueous phases containing metal ions for one

hour at *T*=298.15 K, *T* being controlled by a water bath. After centrifugation, the two phases were separated and aliquots of each phase were sampled for analysis. Nitric acid concentrations in the aqueous and organic phases were measured by acid-base titration against 0.1 M NaOH solution, by diluting the aliquot in water and water/ethanol mixture (50/50%$_{vol}$) respectively or in saturated ammonium oxalate in presence of uranium. Uranium concentration in both phases was determined by UV-vis spectrophotometry (CARY 500 from AGILENT) while ^{99m}Tc activities were measured by gamma spectrometry (Hyper pure Ge detector, CANBERRA). The distribution ratio of technetium (D_{Tc}) is defined according to equation (1):

$$D_{Tc} = \overline{A_{Tc}}/A_{Tc} \quad (1)$$

where $\overline{A}$ and A are the γ radioactivities of ^{99m}Tc, in the organic and aqueous phase respectively (expressed in terms of decays per volume unit per second). It is assumed from previous experiments that D-values between 0.1 and 10 exhibit a maximum error of about 5% while the error may be up to 10% for lower (0.01-0.1) and higher (10-100) values.

Infrared spectroscopy

Table 1 summarizes the compositions of the different samples used for EXAFS and IR experiments. Infrared measurements were performed on the organic samples 1, 2 and 3' using a Bruker Equinox 55 FT-IR spectrometer equipped with an attenuated total reflectance cell. The samples were prepared by solvent extraction following the procedure described above. All spectra were collected between 650 and 4000 cm^{-1} using 32 scans and a resolution of 2 cm^{-1}.

XAS data acquisition

EXAFS spectra for organic samples 1, 2, 3 and 4 (see **Table 1** for experimental conditions) were recorded at the European Synchrotron Radiation Facility (ESRF, Grenoble, France) (6 GeV at 200 mA), at the Rossendorf beamline (BM20), dedicated to radioactive samples analysis.

BM20 is equipped with a water-cooled Si(111) double crystal monochromator (DCM). Beam collimation and rejection of higher-order harmonics were achieved with two Pt-coated cylindrical-shaped mirrors before and after the DCM. A 13-element Ge solid state detector (CANBERRA) was used for data collection in fluorescence mode.

Monochromator energy calibration was carried out using an yttrium metallic foil for uranium L_3 edge (Y K edge at 17038 eV) and a molybdenum foil for technetium K edge (Mo K edge at 20000 eV).

All measurements were performed at room temperature in 200 µL double layered cells specifically designed for radioactive samples. [20] The data represent averages of 4 scans at uranium L_3 edge and 3 to 5 scans for technetium K edge.

Table 1. Summary of the compositions of EXAFS and FT-IR samples.

Sample	$[\overline{DEHiBA}]$ mol.L^{-1}	$[\overline{HNO_3}]$ mol.L^{-1}	$[\overline{U}]$ mol.L^{-1}	$[\overline{Tc}]$ mol.L^{-1}
1	1	$9.62\ 10^{-2}$	$3.65\ 10^{-2}$	0
2	1	$8.57\ 10^{-2}$	$4.24\ 10^{-2}$	$2.60\ 10^{-2}$
3	1	$6.27\ 10^{-2}$	$1.69\ 10^{-2}$	$4.07\ 10^{-2}$
3’	1	$8.57\ 10^{-2}$	$4.24\ 10^{-2}$	$5.20\ 10^{-2}$
4	1	$7.81\ 10^{-2}$	0	$4.20\ 10^{-3}$

CALCULATIONS

Distribution data modeling

Theory

The technetium extraction mechanism was assumed to be similar between TBP and DEHiBA. Hence, in the presence of uranium, technetium can be extracted in at least two different ways as shown by the following equilibriums:

$$i\bar{L} + (j+k)H^+ + kTcO_4^- + jNO_3^- \leftrightharpoons \overline{L_i(HNO_3)_j(HTcO_4)_k} \quad (2)$$

$$\overline{L_i(UO_2(NO_3)_2)_l(HNO_3)_j} + kl\,HTcO_4 \leftrightharpoons \overline{L_i(UO_2(NO_3)_{2-k}(TcO_4)_k)_l(HNO_3)_j} + kl\,HNO_3 \quad (3)$$

where the overlined species refer to the organic phase (L= DEHiBA).

If the thermodynamic constants associated with these reactions are $K^{\circ}_{\bar{C}}$, then:

$$K^{\circ}_{\overline{L_i(HNO_3)_j(HTcO_4)_k}} = \frac{a_{\overline{L_i(HNO_3)_j(HTcO_4)_k}}}{a_{\bar{L}}^{i}\ a_{HNO_3}^{j}\ a_{HTcO_4}^{k}} \quad (4)$$

$$K^{\circ}_{\overline{L_i(UO_2(NO_3)_{2-k}(TcO_4)_k)_l(HNO_3)_j}} = \frac{a_{\overline{L_i(UO_2(NO_3)_{2-k}(TcO_4)_k)_l(HNO_3)_j}}\ a_{HNO_3}^{kl}}{K^{\circ}_{\overline{L_i(UO_2(NO_3)_2)_l(HNO_3)_j}}\ a_{\bar{L}}^{i}\ a_{HNO_3}^{j}\ a_{HTcO_4}^{kl}\ a_{UO_2(NO_3)_2}^{l}} \quad (5)$$

where a_X and $a_{\bar{X}}$ are thermodynamic activities of species, respectively in the aqueous and organic phases. The stoichiometric coefficients of DEHiBA, nitric acid, pertechnetic acid and uranyl nitrate in organic complexes are respectively i, j, k and l.

Deviation from ideal behavior in aqueous solutions

Simple solution theory can be used to take into account deviation from ideal behavior in aqueous solutions. The simple solution concept is stated by the Zdanovskii-Stokes-Robinson relation (ZSR rule) which associates the concentrations of the constituent electrolytes with their concentrations in a binary solution of the same water activity as the mixture: [15]

$$\sum_X m_X/m_X^{bi} = 1 \qquad \text{at } a_{H2O} = \text{cst} \quad (6)$$

where m_X is the molality (mol.kg^{-1}) of the electrolyte X in the mixture, m_X^{bi} is the molality (mol.kg^{-1}) of the electrolyte X in a binary solution of the same water activity as the mixture and a_{H2O} is the water activity of the mixture.

As binary data are available for the solutes HNO_3 [21], $UO_2(NO_3)_2$ [22, 23] and $HTcO_4$ [19] and the $H_2O/HNO_3/UO_2(NO_3)_2$ and $H_2O/HNO_3/HTcO_4$ mixtures are considered to satisfy the "simple" solution concept [23], the ZSR relation can be applied directly to calculate the water activity of the

mixture iteratively. [15] Moreover, for mixtures for which this rule can be applied, Mikulin demonstrated that the activity coefficients of electrolytes can be expressed as a function of the mixture composition and the composition of binary mixtures of the same water activity: [15]

$$\gamma_{st,X} = \nu_X m_X^{bi} \gamma_X^{bi} \Big/ \sum_X \nu_X m_X \quad (7)$$

where $\gamma_{st,X}$ and γ_X^{bi} are the mean stoichiometric activity coefficients of the electrolyte X, respectively in the mixture and in the isopiestic binary solution, m_X and $m_X{}^{bi}$ are the molalities (mol.kg^{-1}) of the electrolyte, in the mixture and in the isopiestic binary solution respectively, ν_X is the sum of the stoichiometric coefficients of the electrolyte. Binary data for nitric acid [21], uranyl nitrate [23] and pertechnetic acid [19] are available in the literature.

Method of modeling

All the calculations for extraction isotherm modeling were performed using the Scilab 5.4.1 software. The calculated concentrations are determined by an iterative method based on least-squares analysis. The following criterion was minimized by comparing the experimental values of the molal concentration with the values calculated by the model:

$$\chi^2 = \sum_X \left(\left(m_{\overline{X},calc} - m_{\overline{X},exp} \right) / m_{\overline{X},exp} \right)^2 \quad (8)$$

Experimental uranium, technetium and nitric acid concentrations in both phases were determined at equilibrium, as described in the experimental section. These results were used to calculate water, nitric acid, uranium and technetium thermodynamic activities in the aqueous phase. Water activity was calculated by an iterative method based on dichotomy resolution of equation (6). The molal concentration of each solvate $m_{\overline{\mathbb{C}}}$ ($\mathbb{C}$ = organic complexes) and the total molal concentrations of technetium ($m_{\overline{Tc}}$), nitric acid ($m_{\overline{HNO_3}}$), DEHiBA ($m_{\overline{DEHiBA}}$) and water ($m_{\overline{H_2O}}$) in the organic phase were calculated with Scilab according to the mass action law and

mass balances associated with each component. To model the extraction isotherms, different hypotheses on the stoichiometry of the organic complexes, consistent with previous published results [24] were put forward. The stoichiometry selected for the model was the one which gave the best agreement between experimental and calculated concentrations, corresponding to the minimum value of χ^2.

DFT calculations

Geometries of uranyl complexes were optimized at the DFT level with the Gaussian 09 software. [25] Becke's hybrid functional (B3LYP) was employed. Optimized geometries were characterized by harmonic frequency analysis as local minima. Calculations were done in the presence of a continuum solvent model. For uranium, the small-core relativistic effective core potential (RECP) and the corresponding basis set suggested by Dolg et al. were used. [26-28] A 6-31+G(d,p) basis set was employed for other atoms.

To reduce computational time, DEHiBA was replaced by DEBiBA (*N,N*-di-2-ethylbutyl-isobutyramide) with slightly shorter alkyl chains on the nitrogen atoms.

XAS data treatment

XAS data processing was carried out with the Athena code. [29] After energy calibration, the E_0 energy was set at the maximum of the absorption edge for uranium: 17177.9 eV, and 21070 eV for technetium (to minimize ΔE_0 in the fitting procedure). The EXAFS signal was extracted by subtracting a linear pre-edge background and a combination of cubic spline functions for atomic absorption background and then normalized by the Lengeler-Eisenberg procedure. Pseudo-radial distribution functions (PRDF) were obtained by Fourier transform in $k^3\chi(k)$ using the ATHENA code [29] between 2 and 13 $Å^{-1}$ for technetium samples and between 2.5 and 17 $Å^{-1}$ for uranium

ones. The R factor (%) and the quality factor (QF, reduced chi^2) of the fits are provided from ARTEMIS. [29]

Back-scattering amplitude and phase shift function were obtained from FEFF 8.2 calculation [30] performed on two model structures. The $\overline{L_2(UO_2)(NO_3)_2}$ model is taken from single crystal XRD [20] and the $\overline{L_2(UO_2)(NO_3)(TcO_4)}$ model from the optimized DFT structures (see DFT section). At the uranium L_3 edge, all fitting operations are performed in R-space over individual radial distances for each ligand (ΔR_{Oyl}, ΔR_{DEHiBA}, ΔR_{NO3}, ΔR_{TcO4}) and Debye-Waller factors (σ^2_{Oyl}, σ^2_{DEHiBA}, σ^2_{NO3}, σ^2_{TcO4}). To take into account the distribution data model, NO_3 and TcO_4 coordination numbers were also adjusted. Coordination numbers for oxygen atoms from uranyl and DEHiBA and amplitude reduction factors (S_0^2) were fixed (2, 2 and 1 respectively). For the technetium K edge, only the $\overline{L_2(UO_2)(NO_3)(TcO_4)}$ model from the optimized DFT structures was used. Only the first coordination shell was considered in the fitting procedure with four oxygen atoms (N_O, ΔR_O and σ^2_O). The amplitude reduction factor was fixed to one.

RESULTS

Modeling results

Extraction of water, nitric acid and uranium by DEHiBA

The data given in reference [13] were used for modeling water, nitric acid and uranium(VI) extraction by DEHiBA (see **Figure 2** and **Figure 3**).

For water extraction by DEHiBA in the absence of nitric acid and uranium, the best agreement between experimental and calculated water concentrations in the organic phase was obtained by considering extraction of the hydrated complex $\overline{(DEHiBA)(H_2O)}$.

For nitric acid and water extraction by DEHiBA in the absence of uranium, the best isotherms modeling was obtained by considering the extraction of three acidic complexes

$\overline{(DEHiBA)_2(HNO_3)(H_2O)}$, $\overline{(DEHiBA)(HNO_3)}$ and $\overline{(DEHiBA)(HNO_3)_2(H_2O)}$ in addition to the species mentioned above for water extraction. Condamines and Musikas [9] described a complete study combining distribution ratio measurements with IR spectroscopy and proposed a mechanism involving the competing formation of these three adducts for HNO_3 extraction by DEHiBA 1 M.

For the $UO_2(NO_3)_2/HNO_3/H_2O$/DEHiBA/TPH system, the best extraction isotherms modeling is obtained by consideration of two complexes $\overline{(DEHiBA)_2(UO_2)(NO_3)_2}$ and $\overline{(DEHiBA)_3(UO_2)(NO_3)_2(HNO_3)}$ in addition to the species mentioned above. D-values increase with nitric acid concentration in the aqueous phase because of the salting-out effect. According to Condamines and Musikas [10], the $\overline{(DEHiBA)_2(UO_2)(NO_3)_2}$ species is assumed to be formed in the organic phase after ligand dependency experiments. However, even if less than 50% of uranyl is under this form in the organic phase, the $\overline{(DEHiBA)_3(UO_2)(NO_3)_2(HNO_3)}$ complex has to be taken into account as well to correctly fit uranium extraction data at high nitric acid concentration in our work.

The complexes and the corresponding parameter associated with the extraction equilibria are reported in **Table 2**. These values were then held fixed when modeling technetium extraction isotherms.

Table 2. Optimized parameters for $H_2O/HNO_3/UO_2(NO_3)_2$/DEHiBA/TPH system

Species	$\mathbf{K}^{\circ}_{\bar{\mathbb{C}}}$
$\overline{(DEHiBA)(H_2O)}$	$7.13\ 10^{-2}$
$\overline{(DEHiBA)_2(HNO_3)(H_2O)}$	$4.20\ 10^{-2}$
$\overline{(DEHiBA)(HNO_3)}$	$1.06\ 10^{-1}$
$\overline{(DEHiBA)(HNO_3)_2(H_2O)}$	$5.77\ 10^{-5}$

$\overline{(DEHiBA)_2(UO_2)(NO_3)_2}$	$6.95\ 10^{-1}$
$\overline{(DEHiBA)_3(UO_2)(NO_3)_2(HNO_3)}$	$3.32\ 10^{-2}$

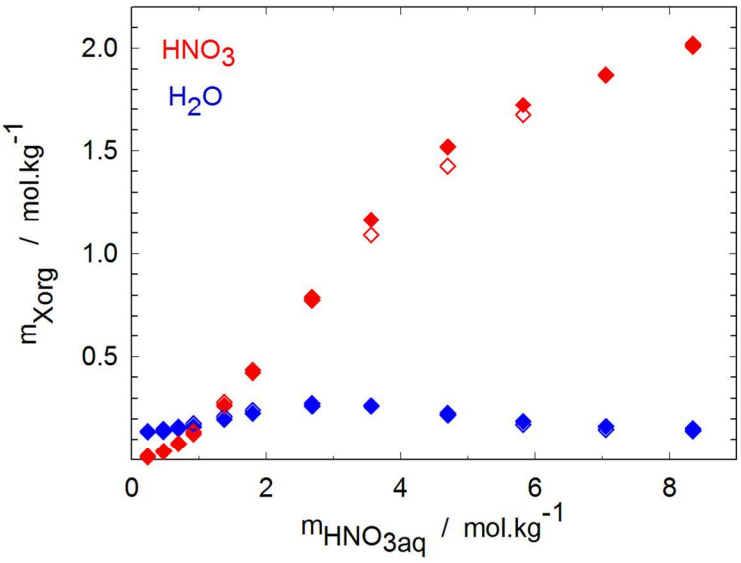

Figure 2. Experimental (♦) and calculated (◊) water and nitric acid organic molalities as a function of nitric acid concentration in the aqueous phase for the H_2O/HNO_3/DEHiBA/TPH system at T=298.15. [DEHiBA] = 1 $mol.L^{-1}$

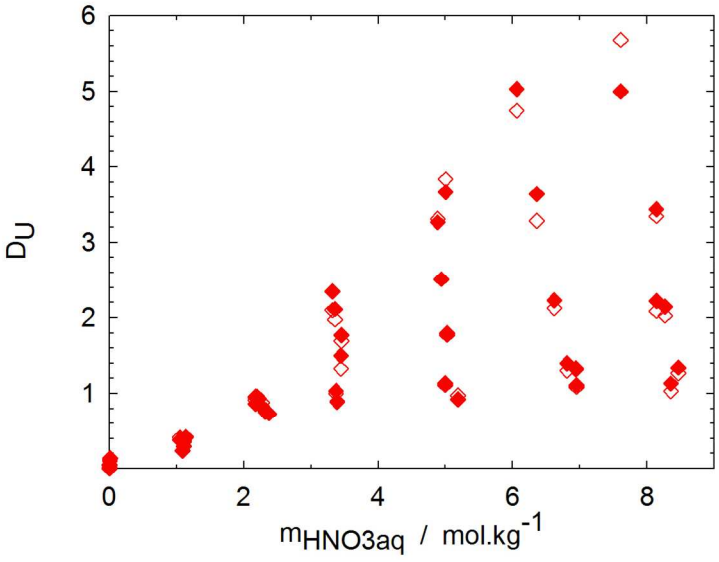

Figure 3. Experimental (♦) and calculated (◊) uranium distribution ratios as a function of nitric acid concentration in the aqueous phase and total uranium concentration for the $H_2O/HNO_3/UO_2(NO_3)_2$/DEHiBA/TPH system at T=298.15. [DEHiBA] = 1 mol.L^{-1}

Technetium extraction by DEHiBA

The Tc(VII) distribution ratio is reported in **Figure 4** as a function of nitric acid molality for different total uranium concentrations.

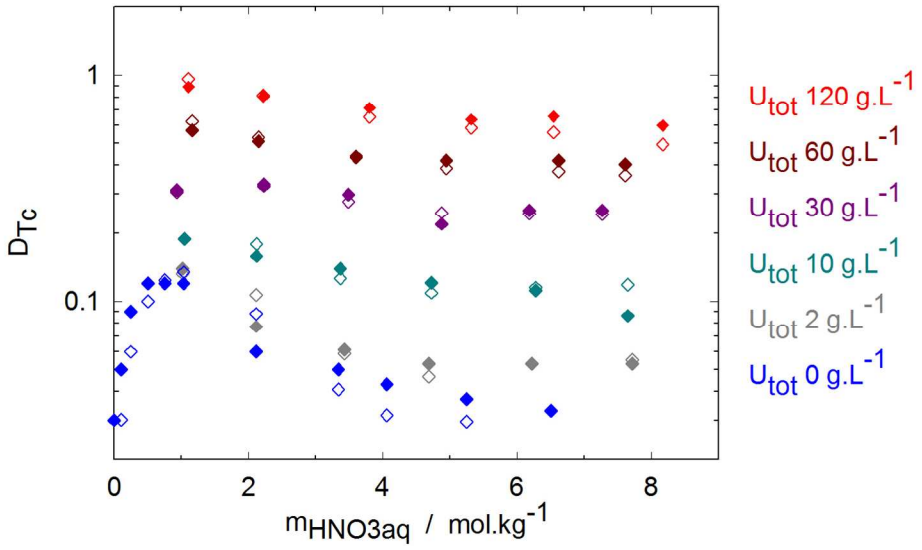

Figure 4. Experimental (♦) and calculated (◊) technetium distribution ratios as a function of nitric acid concentration in the aqueous phase and total uranium concentration for the $H_2O/HNO_3/UO_2(NO_3)_2/HTcO_4$/DEHiBA/TPH system at T=298.15. [DEHiBA] = 1 mol.L^{-1}, [^{99}Tc]=10^{-3} mol.L^{-1} spiked with ^{99m}Tc.

Without uranium, differences in the trend of D_{Tc} occur with the increase in nitric acid concentration. First, the distribution ratio increases with HNO_3 until a maximum near 1 M HNO_3 was reached. Beyond this concentration, more nitric acid is extracted into the organic phase, reducing the concentration of free DEHiBA available and decreasing technetium extraction. This maximum occurs at slightly higher acidity than with TBP 30%$_{vol}$, because water and nitric acid

are less extracted with DEHiBA than with TBP. [31] In the present study, it was possible to correctly model technetium extraction by DEHiBA from these experimental data by taking into account three organic species, in addition to those already mentioned in **Table 2**. The nature of the complexes selected for the modeling and their corresponding extraction constant $K^{\circ}_{\bar{\mathbb{C}}}$ are reported in **Table 3**.

Table 3. Optimized parameters for $H_2O/HNO_3/HTcO_4$/DEHiBA/TPH system

Species	$\mathbf{K}^{\circ}_{\bar{\mathbb{C}}}$
$\overline{(DEHiBA)_4(HTcO_4)}$	$4.71\ 10^{-2}$
$\overline{(DEHiBA)_3(HTcO_4)(HNO_3)}$	$9.39\ 10^{-5}$
$\overline{(DEHiBA)_2(HTcO_4)(HNO_3)}$	$1.27\ 10^{-3}$

The technetium speciation diagram (**Figure 5**) shows the predominance of the $\overline{(DEHiBA)_4(HTcO_4)}$ complex at low to moderate acidities. After 4 $mol.kg^{-1}$, the $\overline{(DEHiBA)_2(HTcO_4)(HNO_3)}$ complex is predominant and the $\overline{(DEHiBA)_3(HTcO_4)(HNO_3)}$ complex is present (even if its proportion remains lower than 10%). This result is consistent with previously published results. [24]

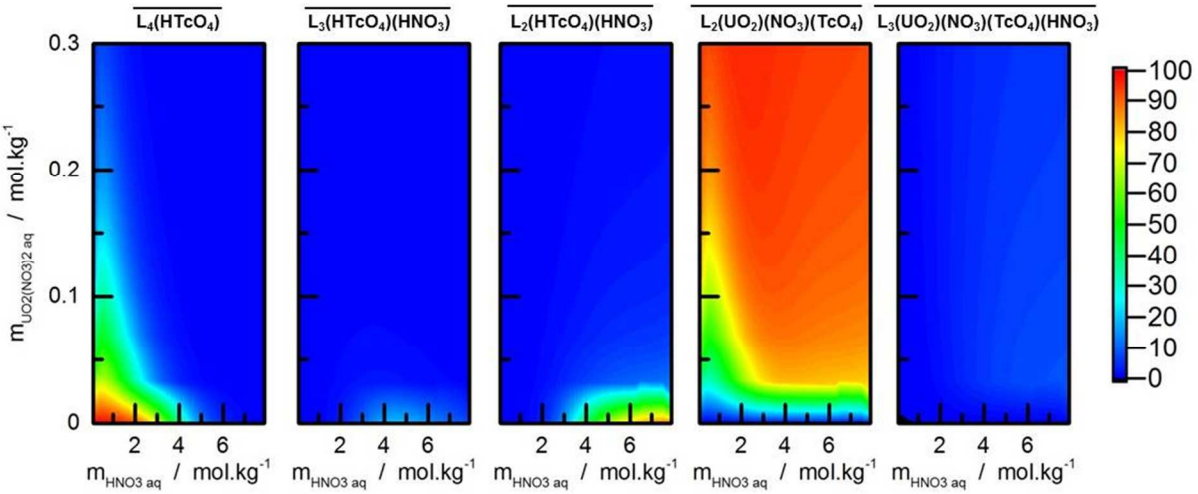

Figure 5. Calculated technetium speciation diagram (in %) for the $H_2O/HNO_3/UO_2(NO_3)_2/HTcO_4$/DEHiBA/TPH system at T=298.15 K as a function of uranium and nitric acid concentrations in the aqueous phase (in mol.kg^{-1}). L=DEHiBA at 1 mol.L^{-1}

In presence of uranium, **Figure 4** clearly shows the increase of Tc extraction as a function of the uranium concentration in the organic phase. This is explained by the co-extraction of TcO_4^- ion with the uranyl complex. Indeed, for high a uranium/technetium ratio, most of the DEHiBA will be present as $\overline{(DEHiBA)_2(UO_2)(NO_3)_2}$, and reaction (2) would be negligible while reaction (3) would become dominant for technetium extraction. The same methodology was used to represent technetium extraction in these conditions and a very good agreement was obtained between calculated and experimental values considering the formation of two mixed complexes $\overline{(DEHiBA)_2(UO_2)(NO_3)(TcO_4)}$ and $\overline{(DEHiBA)_3(UO_2)(NO_3)(TcO_4)(HNO_3)}$ in addition to the complexes mentioned above. Their extraction constants, $K^{\circ}_{\bar{\mathbb{C}}}$, are reported in **Table 4**.

Table 4. Optimized parameters for $H_2O/HNO_3/UO_2(NO_3)_2/HTcO_4$/DEHiBA/TPH system

Species	$\mathbf{K}^{\circ}_{\bar{\mathbb{C}}}$
$\overline{(DEHiBA)_2(UO_2)(NO_3)(TcO_4)}$	12.18
$\overline{(DEHiBA)_3(UO_2)(NO_3)(TcO_4)(HNO_3)}$	4.34

The speciation of technetium is reported in **Figure 5** as a function of nitric acid concentration in the aqueous phase and total uranium concentration. When uranium concentration in the aqueous phase is lower than 0.025 mol.kg^{-1} (i.e. ≈ 5 g.L^{-1}), the technetium speciation is strongly influenced by the nitric acid concentration. As the uranium concentration increases, the$\overline{(DEHiBA)_4(HTcO_4)}$, $\overline{(DEHiBA)_3(HTcO_4)(HNO_3)}$ and $\overline{(DEHiBA)_2(HTcO_4)(HNO_3)}$ proportions slightly decrease in favor of the $\overline{(DEHiBA)_2(UO_2)(NO_3)(TcO_4)}$ species. The calculated technetium speciation map (**Figure 3Figure 5**) clearly shows that, in the presence of a

large amount of uranium, most of the technetium should be extracted as $\overline{(DEHiBA)_2(UO_2)(NO_3)(TcO_4)}$ (> 80% for the more concentrated uranium samples).

Speciation studies

To complete the thermodynamic study and confirm the assumptions deduced from the mathematical fit, fine characterization of the organic phase was achieved using a combination of several spectroscopic techniques coupled with theoretical calculations.

Infrared spectroscopy

From infrared spectroscopy, information can be obtained about carbonyl, nitrate and uranyl stretching vibrations. The infrared spectra of DEHiBA-uranyl nitrato-pertechnetate complexes were compared with those of DEHiBA-uranyl nitrato complexes. **Table 5** summarizes the principal vibrational frequencies of the DEHiBA-uranyl nitrato complexes. [32] As shown in **Figure 6**, the asymmetric stretching frequency of UO_2^{2+} ion occurs at 935 cm^{-1} in the DEHiBA-uranyl nitrato complex. When uranium and technetium are co-extracted, no significant change is observed but a slight shift of the carbonyl C=O stretch (from 1572 to 1564 cm^{-1}) is noticed when the Tc/U ratio increases.

Table 5. Selected vibrational frequencies of the DEHiBA-uranyl nitrato complexes

Type of vibration	ν / cm^{-1}
ν free C=O	1650
ν bonded C=O	1573
ν_1 N=O	1525
ν_4 N-O	1272
ν_2 N-O	1029
ν_{as} UO_2^{2+}	935

ν N-O	745

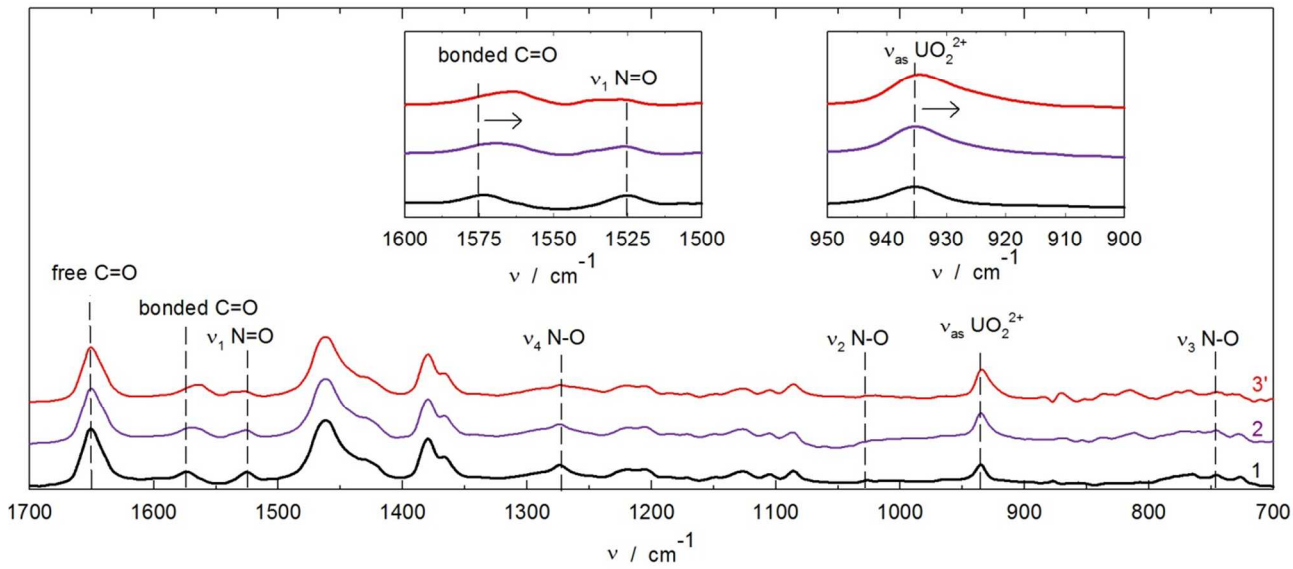

Figure 6. Infrared spectra for samples 1 (DEHiBA-uranyl nitrato complexes, $[\overline{Tc}]/[\overline{U}]=0$), 2 and 3' (DEHiBA-uranyl pertechnetate nitrato complexes, $[\overline{Tc}]/[\overline{U}]=0.6$ and 1.2 respectively). See Table 1 for the sample compositions.

Varying the Tc/U ratio also induces some changes in the intensity and in the shape of the nitrate ν_1 N=O stretch. The changes observed, although very weak, suggest that modifications in the immediate uranyl coordination environment occur with an increase of Tc concentration in the organic phase.

DFT calculations

DFT calculations were undertaken to further investigate the coordination geometry in the inner coordination sphere of uranium.

Geometries of $\overline{(DEHiBA)_2(UO_2)(NO_3)(TcO_4)}$ were optimized and compared to $\overline{(DEHiBA)_2(UO_2)(NO_3)_2}$. In a previous study, it was shown that in the absence of Tc, uranyl is

surrounded by two DEHiBA and two bidentate nitrate ions. [20, 33] Initial structures were constructed where TcO_4^- replaces one nitrate ion in a bidentate coordination mode. However, in the course of the geometry optimization, TcO_4^-, which is bulkier than NO_3^-, becomes monodentate. The resulting optimized geometry and structural parameters are shown in **Figure 7** and **Table 6** for both complexes.

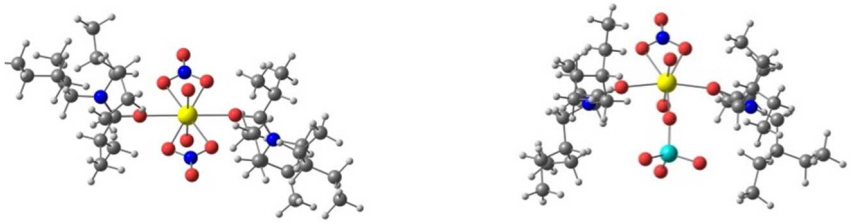

Figure 7. Optimized structures of the $\overline{(\mathrm{DEHiBA})_2(\mathrm{UO_2})(\mathrm{NO_3})_2}$ (left) and $\overline{(\mathrm{DEHiBA})_2(\mathrm{UO_2})(\mathrm{NO_3})(\mathrm{TcO_4})}$ (right) complexes

Table 6. Calculated selected distances (average values in Å) and vibrational frequencies (in cm^{-1}) in $\overline{(\mathrm{DEHiBA})_2(\mathrm{UO_2})(\mathrm{NO_3})_2}$ and $\overline{(\mathrm{DEHiBA})_2(\mathrm{UO_2})(\mathrm{NO_3})(\mathrm{TcO_4})}$ from DFT/B3LYP in heptane (vibrational frequencies calculated in water solvent model in parentheses)

	$\overline{(\mathrm{DEHiBA})_2(\mathrm{UO_2})(\mathrm{NO_3})_2}$	$\overline{(\mathrm{DEHiBA})_2(\mathrm{UO_2})(\mathrm{NO_3})(\mathrm{TcO_4})}$
U=O	1.77	1.77
U-O(DEHiBA)	2.40	2.36
U-O(NO_3)	2.54	2.52
U-O(TcO_4))	-	2.33
U-Tc	-	3.99
ν bonded C=O	1606 (1587)	1589 (1576)
ν_{as} UO_2^{2+}	947 (933)	947 (930)

Vibrational frequencies were computed for the two species. Values for C=O stretching and uranyl asymmetric stretching frequencies are given in **Table 6**. Calculations were performed in

the presence of a continuum solvent model corresponding to heptane and water. The dielectric constant of the organic solution is not known, but should be in between heptane and water. As shown in **Table 6**, vibrational frequencies are strongly influenced by the dielectric constant of the solvent model. Regardless, similar trends are obtained in both media: the carbonyl stretching frequency is redshifted by 11 to 17 cm^{-1} while the uranyl stretching frequency is not significantly shifted in the presence of a monodentate TcO_4^-. These variations are consistent with experimental spectra and with the presence of TcO_4^- in the coordination sphere of uranium. Calculated distances are not significantly altered by the solvent model and only values in heptane are reproduced. Uranium-oxygen distances in the equatorial plane are slightly shortened by 0.02 to 0.04 Å in the presence of TcO_4^-. This is due to the monodentate coordination mode of TcO_4^- which decreases the uranyl coordination number from 6 to 5.

EXAFS data analysis

The technetium and uranium absorption edge shape and edge position (chemical shift) can be used to confirm (i) the local structure of the absorbing atoms and (ii) the oxidation state of the absorbing atoms.

The technetium edges were identical for all samples and very similar to the published data for the pertechnetate species. [34] The intense pre-edge observed at 21050 eV is due to 1s → nd transition only observed in tetrahedral geometry. Moreover the maximum edge energy at 21090 eV is consistent to previous results for TcO_4 compounds in solid state or aqueous phases. [34, 35]

For uranium, the maximum intensity of the absorption edge at 17177 eV is consistent with U(VI). After the intense white line, two other features at (17192 eV and 17210 eV) are observed respectively due to resonant scattering along the linear transdioxo unit (UO_2^{2+}) and to atoms in the equatorial plan. [36]

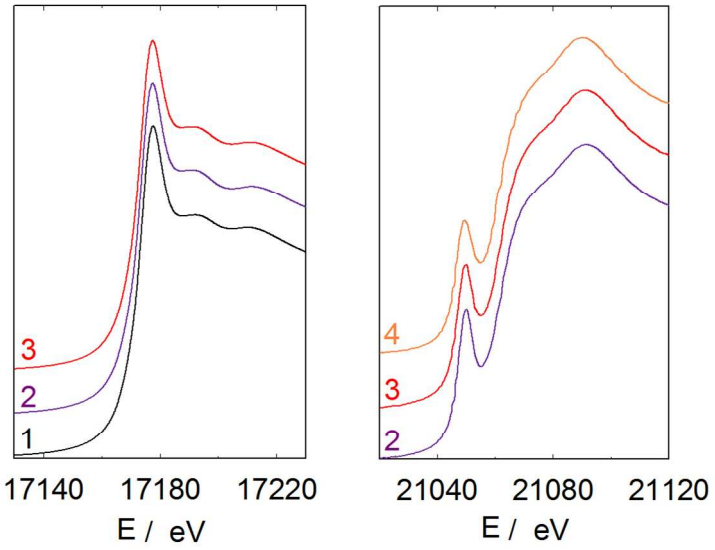

Figure 8. Uranium L_3 (left) and technetium K (right) absorption edges for sample 1, 2, 3 and 4.

Besides the edge itself, the extended fine structures (EXAFS) were used to determine the technetium and uranium first and second coordination shell.

For technetium K edge, EXAFS spectra $\chi(k)\cdot k^3$ and corresponding Fourier transforms (with fits) are presented in the Supporting Information, and the fit results are listed in **Table 7**. Both coordination numbers of the oxygen atoms (4) and Tc=O distance (1.73 Å) are consistent with the pertechnetate geometry. [35] Nevertheless, the Tc-U distance at 3.60 Å proposed by Suzuki et al [17] in co-extracted U/Tc complexes in TBP media is not observed.

The k^3-weighted Fourier transforms of EXAFS spectra obtained for samples 1, 2 and 3 for uranium L_3 edges are depicted in **Figure 9** (EXAFS spectra $\chi(k)\cdot k^3$ are given in the Supporting Information).

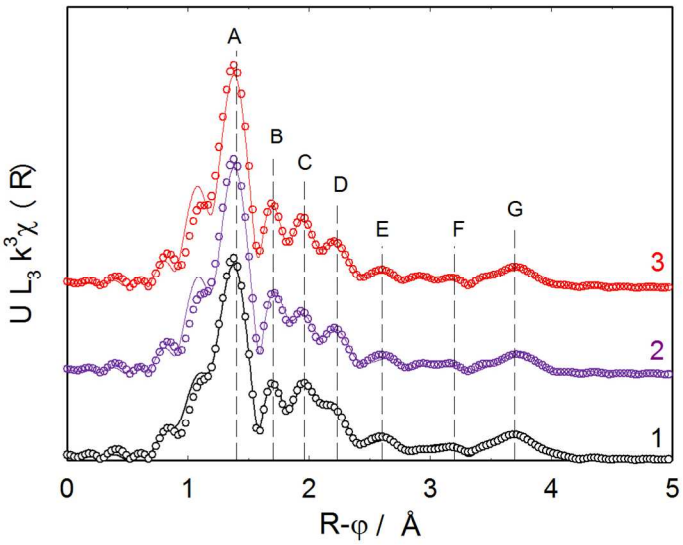

Figure 9. Experimental (—) and fitted (◦◦◦) Fourier transform of the k^3-weighted EXAFS spectra at uranium L_3 edge for organic samples 1 (DEHiBA-uranyl nitrato complexes, $[\overline{Tc}]/[\overline{U}]=0$), 2 and 3 (DEHiBA-uranyl pertechnetate nitrato complexes, $[\overline{Tc}]/[\overline{U}]=0.6$ and 2.4 respectively).

EXAFS oscillations are dominated by the trans-dioxo uranyl bond in the four samples corresponding on the Fourier transform to an intense peak (A) at R+φ = 1.4 Å. Atoms in uranyl equatorial plane result in 3 distinct peaks (B, C and D) observed between R+φ = 1.6 Å and R+φ = 2.5 Å on the Fourier transform. The Tc loading of the samples affects the intensity of peak C suggesting a modification in the uranium first coordination sphere. The second and third coordination shell observed at R+φ > 2.5 Å (peaks E, F and G) are likely related to a uranyl MS effect, DEHiBA C back scattering and bidentate nitrate oxygen atoms.

The spectra were fit according to the procedure described in the calculation section. The theoretical spectra are displayed in **Figure 9** and the fit results are summarized in **Table 7**.

The $\overline{L_2(UO_2)(NO_3)_2}$ model taken from single crystal XRD [20] and the $\overline{L_2(UO_2)(NO_3)(TcO_4)}$ model including pertechnetate bound to uranium in a monodentate fashion were used. To determine the coordination sphere in the four samples, both distances and the Debye Waller

factor were adjusted for each scattering path. Coordination numbers for the monoamide and -yl oxygen were fixed while the nitrate and pertechnetate coordination numbers were interconnected floating parameters ($N_{NO3} = 2 - N_{TcO4}$). For the four samples, this model fit very well with the experimental data with an R-factor ≤ 2%. Distances obtained after data refinement are in agreement with XRD references and DFT models, within error. The two axial -yl oxygen atoms are stable at 1.77 Å while slight changes are observed in the equatorial oxygen shell as shown by direct reading of experimental data. By increasing the Tc loading in the sample, the bidentate nitrate coordination number decreases with a concomitant increase of the monodentate pertechnetate oxygen atom. The result is a decrease of the total coordination number for uranyl equatorial oxygen (6 in sample 1 to 5.7 and 5.3 for the sample 2 and 3 respectively). As a result, the mean uranyl equatorial oxygen distance decreases from 2.48 Å for sample 1 to 2.45 Å for the most Tc loaded sample.

According to the Suzuki et al. [17] EXAFS study on TBP, both pertechnetate and nitrate groups coordinate the uranyl cation in a bidentate fashion. In TBP, the first uranyl coordination shell is maintained (CN=6 and $R\text{-}O_{ax}$ = 2.48 Å) which contrasts with the studied monoamide system. Moreover, the Tc backscattering effect expected at 3.60 Å for bidentate pertechnetate is never observed. In the proposed monodentate model, the Tc is expected at about 4.1 Å (overlapping with the second nitrate oxygen (O'_{NO3}) shell oxygen at 4.2 Å –peak G).

Table 7. EXAFS fit parameters for samples 1 to 4. (*) indicates fixed parameters. (#) indicates interrelated parameters ($N_{U\text{-}O_{NO3}} = 2$ x $(2 - N_{TcO4})$, $N_{U\text{-}N_{NO3}} = 2 - N_{TcO4}$, $N_{U\text{-}O'_{NO3}} = 2 - N_{TcO4,}$, $N_{U\text{-}O_{TcO4}} = N_{TcO4}$ and $N_{U\text{-}Tc} = N_{TcO4}$). Fitting range: 2.5 $Å^{-1}$ to 16.5 $Å^{-1}$ at the U L_3 edge 2 $Å^{-1}$ to 11 $Å^{-1}$ at the Tc K edge.

Technetium	1	2	3	4

Tc K edge	-			$S_0^2 = 1$; $\Delta E^0 = 0.6$ eV; $R_f = 2\%$			$S_0^2 = 1$; $\Delta E^0 = -0.5$ eV; $R_f = 3\%$			$S_0^2 = 1$; $\Delta E^0 = 2.4$ eV; $R_f = 2\%$		
Path	-	-	-	N	σ^2 (Å²)	R (Å)	N	σ^2 (Å²)	R (Å)	N	σ^2 (Å²)	R (Å)
Tc-O	-	-	-	*4.5 (8)*	*0.002**	1.76 (2)	*4.5 (8)*	*0.002**	1.76 (2)	*5.1 (8)*	*0.002**	1.77 (2)

Uranium	**1**			**2**			**3**			**4**		
U L_3 edge	$S_0^2 = 1$; $\Delta E^0 = 4.2$ eV; $R_f = 1\%$			$S_0^2 = 1$; $\Delta E^0 = 4.49$ eV; $R_f = 1\%$			$S_0^2 = 1$; $\Delta E^0 = 4.16$ eV; $R_f = 2\%$			-		
Path	N	σ^2 (Å²)	R (Å)	N	σ^2 (Å²)	R (Å)	N	σ^2 (Å²)	R (Å)	-	-	-
U=O	*2**	*0.002 (1)*	1.77 (1)	*2**	*0.001 (1)*	1.77 (1)	*2**	*0.002 (1)*	1.77 (1)	-	-	-
U-O$_{mono}$	*2**	*0.007 (2)*	2.39 (4)	*2**	*0.005 (2)*	2.38 (1)	*2**	*0.004 (2)*	2.35 (1)	-	-	-
U-O$_{NO3}$	*4.0$^{\#}$ (0.1)*	*0.007 (2)*	2.52 (2)	*3.4$^{\#}$ (2)*	*0.006 (2)*	2.53 (1)	*2.7$^{\#}$ (2)*	*0.006 (2)*	2.51 (2)	-	-	-
U-O$_{TcO4}$	*0.0$^{\#}$ (1)*	-	-	*0.3$^{\#}$ (2)*	*0.009 (3)*	2.51 (3)	*0.6$^{\#}$ (2)*	*0.006 (3)*	2.48 (2)	-	-	-
U-N$_{NO3}$	*2.0$^{\#}$ (1)*	*0.005 (2)*	2.97 (2)	*1.7$^{\#}$ (2)*	*0.006 (2)*	2.95 (3)	*1.4$^{\#}$(2)*	*0.004 (2)*	2.96 (4)	-	-	-
U-C$_{mono}$	*2**	*0.007 (10)*	3.99 (10)	*2**	*0.006 (8)*	3.97 (10)	*2**	*0.010 (8)*	4.00 (10)	-	-	-
U-O'$_{NO3}$	*2.0$^{\#}$(1)*	*0.008 (2)*	4.20 (10)	*1.7$^{\#}$ (2)*	*0.010 (3)*	4.20 (7)	*1.4$^{\#}$ (2)*	*0.010 (4)*	4.20 (6)	-	-	-
U-Tc	*0.0$^{\#}$ (1)*	-	-	*0.3$^{\#}$ (2)*	*0.009 (4)*	4.12 (3)	*0.6$^{\#}$ (2)*	*0.006 (2)*	4.08 (2)	-	-	-

CONCLUSIONS

A full comprehensive study of technetium(VII) extraction by the *N,N*-dialkylamide DEHiBA was performed.

Experimental extraction isotherms were first acquired in batch conditions to evaluate the influence of nitric acid and uranium concentrations on technetium distribution ratios. The increase in technetium extraction with the addition of uranium to the organic phase and the decrease of nitric acid concentration in the aqueous phase were correctly modeled. A thermodynamic approach based on the mass action law and using the simple solution concept to

correct the deviations from ideal solutions in the aqueous phase was used. Without uranium, the presence of three complexes was assumed in the organic phase: $\overline{(\mathrm{DEHiBA})_4(\mathrm{HTcO_4})}$, $\overline{(\mathrm{DEHiBA})_3(\mathrm{HTcO_4})(\mathrm{HNO_3})}$ and $\overline{(\mathrm{DEHiBA})_2(\mathrm{HTcO_4})(\mathrm{HNO_3})}$, while co-extraction of technetium(VII) with uranium(VI) was modeled using $\overline{(\mathrm{DEHiBA})_2(\mathrm{UO_2})(\mathrm{NO_3})(\mathrm{TcO_4})}$ and $\overline{(\mathrm{DEHiBA})_3(\mathrm{UO_2})(\mathrm{NO_3})(\mathrm{TcO_4})(\mathrm{HNO_3})}$ complexes.

To complete the classic thermodynamic description of metal extraction by a neutral extractant and to probe the formation of the $\overline{(\mathrm{DEHiBA})_2(\mathrm{UO_2})(\mathrm{NO_3})(\mathrm{TcO_4})}$ species, the molecular structures were further investigated through spectroscopic measurements and theoretical calculations. FT-IR experiments showed that the uranyl inner sphere was affected by the presence of technetium. DFT calculations predicted that one TcO_4^- anion replaces one nitrate ion in a monodentate coordination mode in the $\overline{(\mathrm{DEHiBA})_2(\mathrm{UO_2})(\mathrm{NO_3})_2}$ complex. EXAFS analysis, supported by theoretical calculations, confirmed the formation of this complex and the inner-sphere coordination mode: a pertechnetate group coordinates the uranyl cation in a monodentate fashion. A previous structural study suggests that during the co-extraction of uranium and technetium by TBP, both pertechnetate and nitrate groups coordinate the uranyl cation in a bidentate fashion. With the monoamide DEHiBA, the pertechnetate group should preferentially coordinate the uranyl cation in a monodentate fashion. Such a monodentate coordination mode should be favored by steric effects induced by the presence of amides with large alkyl groups and TcO_4^- which is bulkier than NO_3^-.

Combining a macroscopic study (distribution data acquisition and modeling) with molecular-scale investigations (FT-IR and X-ray absorption analysis supported by theoretical calculations) has provided a new insight into the description of solvent extraction mechanism. This study shows the interest of investigating speciation both at macroscopic and molecular scales. This set

of complementary methods could also be applied to other extractant systems, especially to observe the influence of the amide structure (branched or linear alkyl chains) on the coordination mode. It will allow for a better simulation of technetium in the solvent extraction process to further master its separation and decontamination in future reprocessing plants.

ACKNOWLEDGEMENTS

The authors are grateful to L. Chareyre and J. Chapelet for their support for ^{99m}Tc experiments, to C. Lefèbvre for support during the EXAFS experiment and to Dr. J. Muller and Dr. J. Drader for the redaction of the paper. The authors express their thanks to Dr. F. Poineau for his explanations and fruitful discussions on the work related to XAS data analysis. Many thanks go to Dr. C. Tamain for her valuable assistance in FT-IR analysis. The authors acknowledge AREVA NC and the European Talisman project for financial support.

ASSOCIATED CONTENT

Supporting Information

The following file is available free of charge.

Superposition of experimental and calculated k^3-weighted EXAFS spectra and Fourier transform of the k^3-weighted EXAFS spectra at uranium L_3 and technetium K edges for organic samples 1 (DEHiBA-uranyl nitrato complexes), 2 and 3 (DEHiBA-uranyl pertechnetate nitrato complexes) (PDF)

REFERENCES

1. K. H. Lieser, A. Krüger and R. N. Singh, *Radiochimica Acta*, 1981, **28**, 97-101.
2. J. G. Darab and P. A. Smith, *Chemistry of Materials*, 1996, **8**, 1004-1021.
3. K. Schwochau, *Technetium: Chemistry and Radiopharmaceutical Applications*, 2000.
4. CEA, *Treatment and recycling of spent nuclear fuel. Actinide partitioning – Application to waste management*, Le moniteur, Gif-sur-Yvette, 2008.
5. T. N. Jassim, G. Persson and J. O. Liljenzin, *Solv. Extr. Ion Exch.*, 1984, **2**, 1079-1092.
6. D. J. Pruett, *Radiochimica Acta*, 1981, **28**, 153-157.
7. T. H. Siddall, *The Journal of Physical Chemistry*, 1960, **64**, 1863-1866.

8. D. J. Pruett, *The solvent extraction of heptavalent technetium and rhenium by tributyl phosphate* ORNL/TM-8668, Tenessee, 1984.
9. N. Condamines and C. Musikas, *Solvent extraction and ion exchange*, 1988, **6**, 1007-1034.
10. N. Condamines and C. Musikas, *Solvent extraction and ion exchange*, 1992, **10**, 69-100.
11. P. N. Pathak, D. R. Prabhu, P. B. Ruikar and V. K. Manchanda, *Solvent extraction and ion exchange*, 2002, **20**, 293-311.
12. T. H. Siddall and M. O. N. Fulda, G. S., *Nuclear technology - Chemistry and chemical engineering*, 1961.
13. M. Miguirditchian, C. Sorel, B. Cames, I. Bisel and P. Baron, *ISEC'08*, 2008.
14. B. Mokili and C. Poitrenaud, *Solvent extraction and ion exchange*, 1995, **13**, 731-754.
15. B. Mokili and C. Poitrenaud, *Solvent extraction and ion exchange*, 1996, **14**, 617-634.
16. F. Macasek and J. Kadrabova, *Journal of Radioanalytical Chemistry*, 1979, **51**, 97-106.
17. S. Suzuki, T. Yaita, Y. Okamoto, H. Shiwaku and H. Motohashi, *Physica Scripta*, 2005, **T115**, 306-307.
18. G. E. Boyd, *Inorganic Chemistry*, 1978, **17**, 1808-1810.
19. P. Moeyaert, L. Abiad, C. Sorel, J. F. Dufrêche, A. Ruas, P. Moisy and M. Miguirditchian, *The Journal of Chemical Thermodynamics*, 2015, **91**, 94-100.
20. E. Acher, Y. Hacene Cherkaski, T. Dumas, C. Tamain, D. Guillaumont, N. Boubals, H. C., P. L. Solari and M. C. Charbonnel, *Inorganic Chemistry*, 2016, http://dx.doi.org/10.1021/acs.inorgchem.6b00592.
21. N. Charrin, P. Moisy, S. Garcia-Argote and P. Blanc, *Radiochimica Acta*, 1999, **86**, 143-149.
22. R. Goldberg, *Journal of Physical and Chemical Reference Data*, 1979, **8**, 1005-1050.
23. A. Ruas, O. Bernard, B. Caniffi, J. P. Simonin, P. Turq, L. Blum and P. Moisy, *Journal of Physical Chemistry B*, 2006, **110**, 3435-3443.
24. N. Kumari, P. N. Pathak, D. R. Prabhu and V. K. Manchanda, *Separation Science and Technology*, 2011, **46**, 79-86.
25. M. J. Frisch, G. W. Trucks, H. B. Schlegel, G. E. Scuseria, M. A. Robb, J. R. Cheeseman, G. Scalmani, V. M. Barone, B., G. A. Petersson, H. Nakatsuji, M. L. Caricato, X., H. P. Hratchian, A. F. Izmaylov, J. Bloino, G. Zheng, J. L. Sonnenberg, M. Hada, M. Ehara, K. Toyota, R. Fukuda, J. Hasegawa, M. Ishida, T. Nakajima, Y. Honda, O. Kitao, H. Nakai, T. Vreven, J. A. Montgomery, Jr., J. E. Peralta, F. Ogliaro, M. Bearpark, J. J. Heyd, E. Brothers, K. N. Kudin, V. N. Staroverov, R. Kobayashi, J. Normand, K. Raghavachari, A. Rendell, J. C. Burant, S. S. Iyengar, J. Tomasi, M. Cossi, N. Rega, J. M. Millam, M. Klene, J. E. Knox, J. B. Cross, V. Bakken, C. Adamo, J. Jaramillo, R. Gomperts, R. E. Stratmann, O. Yazyev, A. J. Austin, R. Cammi, C. Pomelli, J. W. Ochterski, R. L. Martin, K. Morokuma, V. G. Zakrzewski, G. A. S. Voth, P., J. J. Dannenberg, S. Dapprich, A. D. Daniels, Ö. Farkas, J. B. Foresman, J. V. Ortiz, J. Cioslowski and D. J. Fox, *Gaussian, Inc., Wallingford CT*, 2009.
26. X. Y. Cao and M. Dolg, *Journal of Molecular Structure-Theochem*, 2002, **581**, 139-147.
27. X. Y. Cao, M. Dolg and H. Stoll, *Journal of Chemical Physics*, 2003, **118**, 487-496.
28. M. Dolg, H. Stoll, A. Savin and H. Preuss, *Theoretica Chimica Acta*, 1989, **75**, 173-194.
29. B. Ravel and M. Newville, *Journal of Synchrotron Radiation*, 2005, **12**, 537-541.
30. J. J. Rehr and R. C. Albers, *Reviews of Modern Physics*, 2000, **72**, 621-654.
31. S. De Sio, C. Sorel, E. Bosse and P. Moisy, *Radiochimica Acta*, 2013, **101**, 373-377.

32. F. Rodrigues, G. Ferru, L. Berthon, N. Boubals, P. Guilbaud, C. Sorel, O. Diat, P. Bauduin, J. P. Simonin, J. P. Morel, N. Morel-Desrosiers and M. C. Charbonnel, *Molecular Physics*, 2014, **112**, 1362-1374.
33. T. Yaita, H. Narita, S. Suzuki, S. Tachimori, H. Shiwaku and H. Motohashi, *Journal of Alloys and Compounds*, 1998, **271**, 184-188.
34. F. Poineau, M. Fattahi, C. Den Auwer, C. Hennig and B. Grambow, *Radiochimica Acta*, 2006, **94**, 283-289.
35. F. Poineau, P. F. Weck, K. German, A. Maruk, G. Kirakosyan, W. Lukens, D. B. Rego, A. P. Sattelberger and K. R. Czerwinski, *Dalton Transactions*, 2010, **39**, 8616-8619.
36. C. Fillaux, J. C. Berthet, S. D. Conradson, P. Guilbaud, D. Guillaumont, C. Hennig, P. Moisy, J. Roques, E. Simoni, D. K. Shuh, T. Tyliszczak, I. Castro-Rodriguez and C. Den Auwer, *Comptes Rendus Chimie*, 2007, **10**, 859-871.

TOC

The co-extraction mechanism of technetium (VII) in the presence of uranium (VI) by the N,N-dialkyl amide DEHiBA was elucidated. By combining a macroscopic approach (distribution data acquisition and modeling) with molecular-scale investigations (FT-IR and X-ray absorption analysis supported by theoretical calculations), a new insight into the description of solvent extraction mechanism is provided.

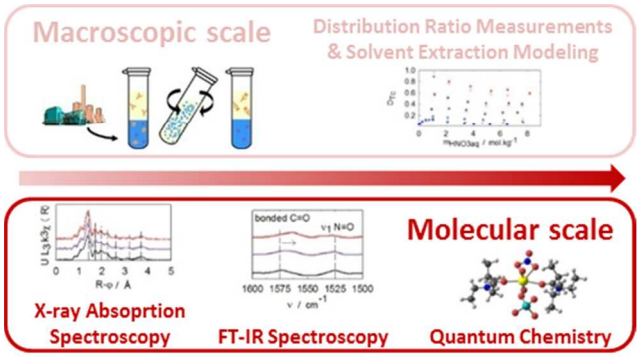

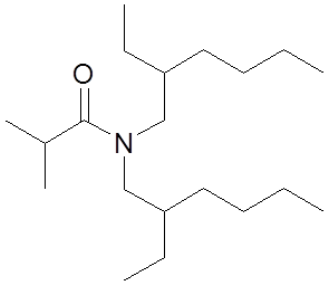

Figure 1. Scheme of *N,N*-di-2-ethylhexyl-isobutyramide (DEHiBA)

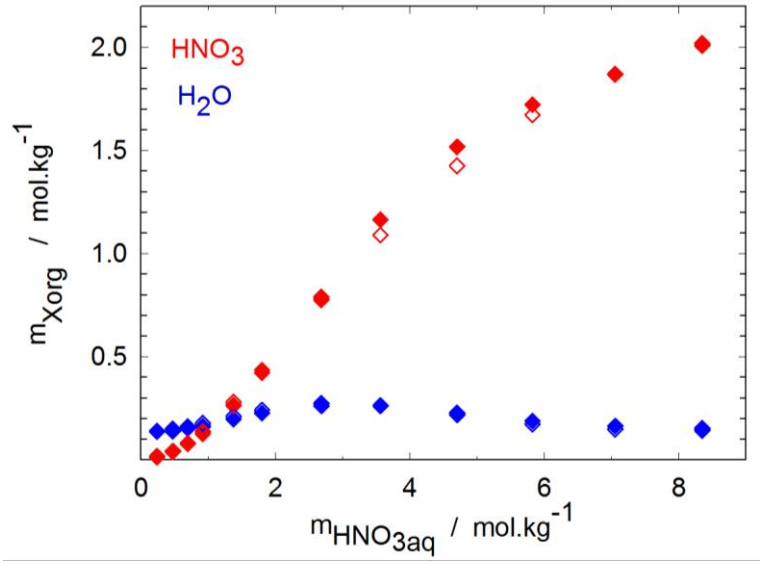

Figure 2. Experimental (♦) and calculated (◊) water and nitric acid organic molalities as a function of nitric acid concentration in the aqueous phase for the H_2O/HNO_3/DEHiBA/TPH system at T=298.15. [DEHiBA] = 1 mol.L^{-1}

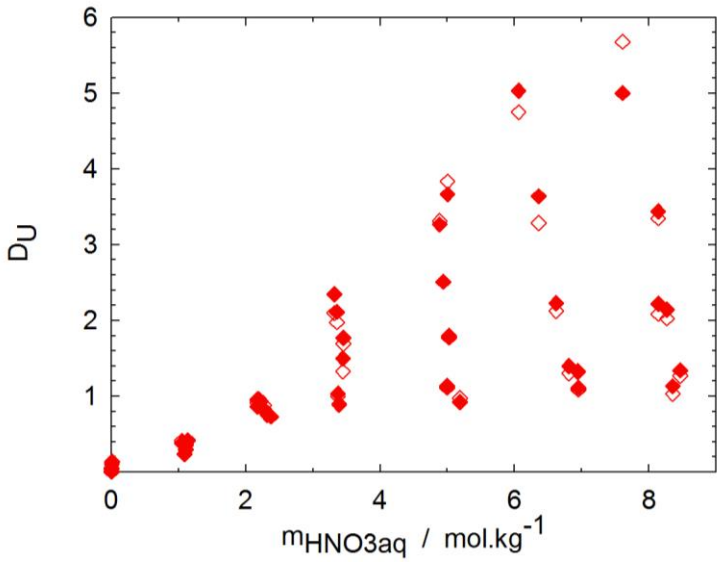

Figure 3. Experimental (♦) and calculated (◊) uranium distribution ratios as a function of nitric acid concentration in the aqueous phase and total uranium concentration for the $H_2O/HNO_3/UO_2(NO_3)_2$/DEHiBA/TPH system at T=298.15. [DEHiBA] = 1 mol.L^{-1}

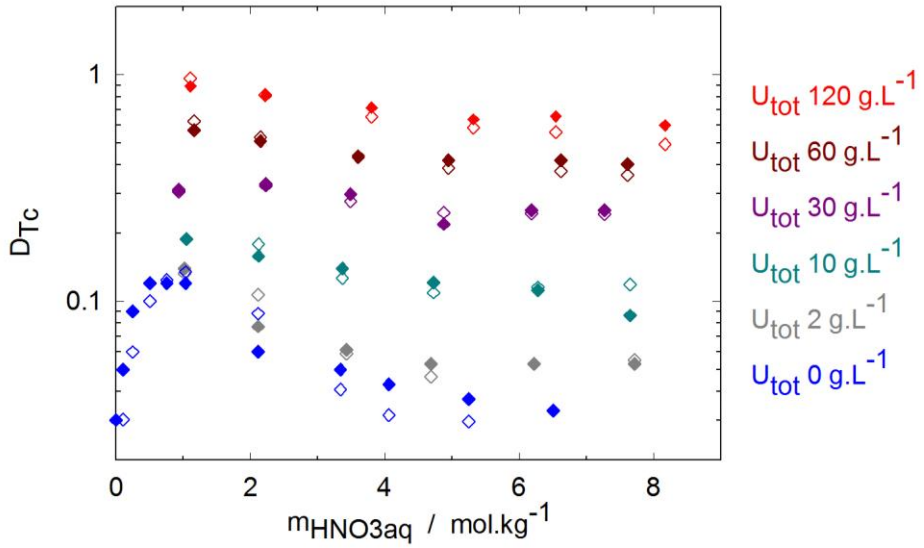

Figure 4. Experimental (♦) and calculated (◊) technetium distribution ratios as a function of nitric acid concentration in the aqueous phase and total uranium concentration for the $H_2O/HNO_3/UO_2(NO_3)_2/HTcO_4$/DEHiBA/TPH system at T=298.15. [DEHiBA] = 1 mol.L^{-1}, [^{99}Tc]=10^{-3} mol.L^{-1} spiked with ^{99m}Tc.

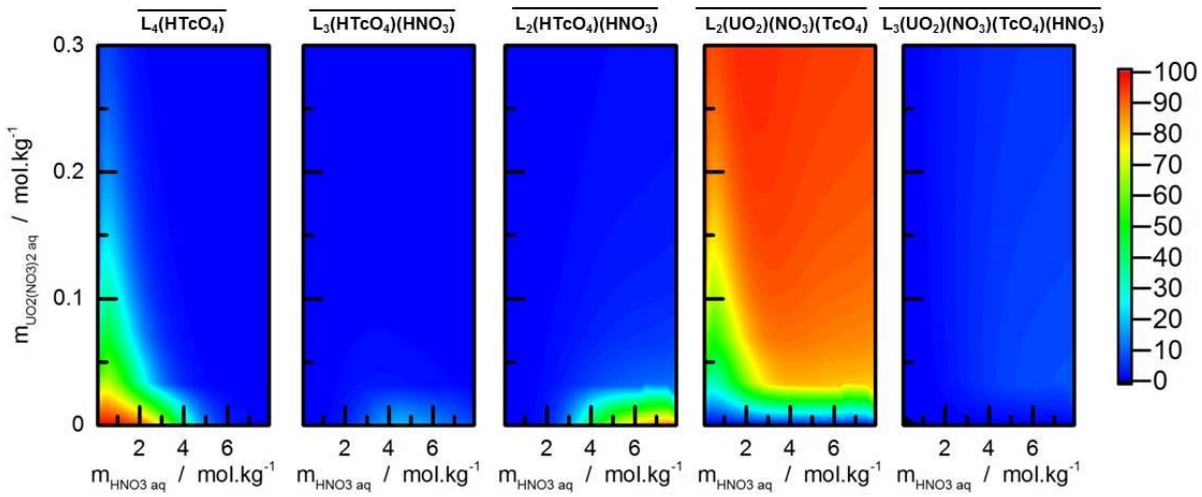

Figure 5. Calculated technetium speciation diagram (in %) for the $H_2O/HNO_3/UO_2(NO_3)_2/HTcO_4$/DEHiBA/TPH system at T=298.15 K as a function of uranium and nitric acid concentrations in the aqueous phase (in mol.kg^{-1}). L=DEHiBA at 1 mol.L^{-1}

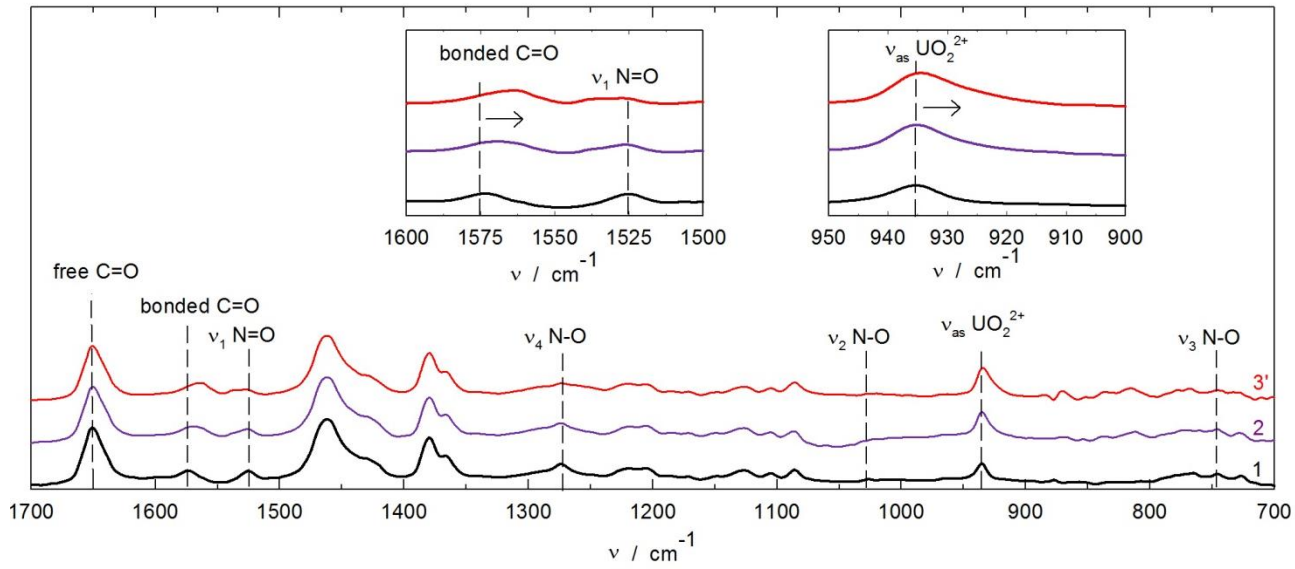

Figure 6. Infrared spectra for samples 1 (DEHiBA-uranyl nitrato complexes, $[\overline{Tc}]/[\overline{U}]$=0

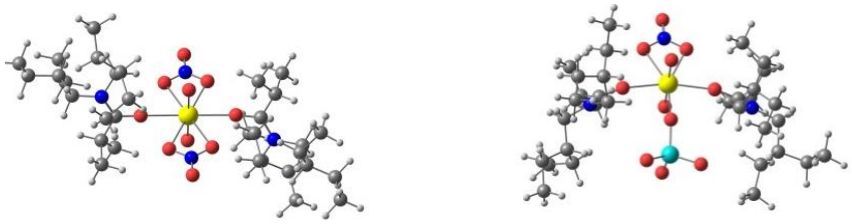

Figure 7. Optimized structures of the $\overline{(\mathrm{DEHiBA})_2(\mathrm{UO_2})(\mathrm{NO_3})_2}$ (left) and $\overline{(\mathrm{DEHiBA})_2(\mathrm{UO_2})(\mathrm{NO_3})(\mathrm{TcO_4})}$ (right) complexes

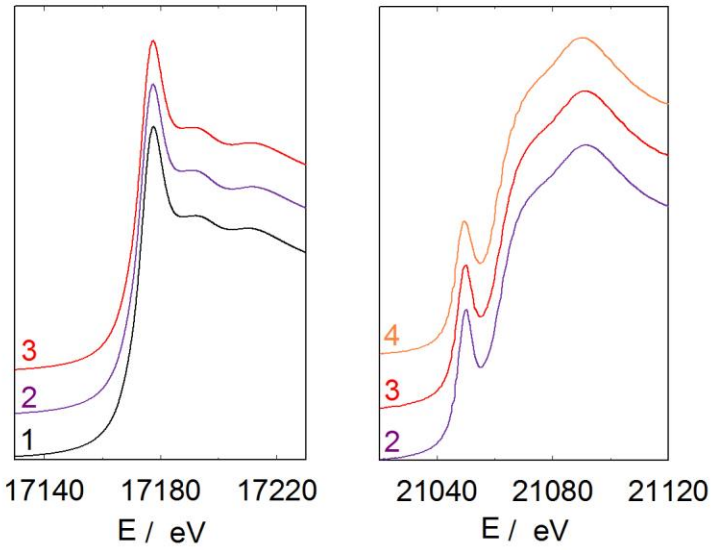

Figure 8. Uranium L_3 (left) and technetium K (right) absorption edges for sample 1, 2, 3 and 4.

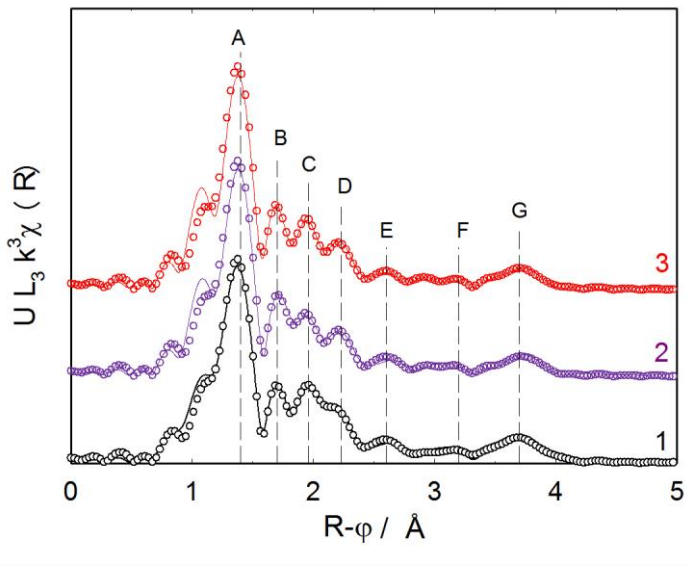

Figure 9. Experimental (—) and fitted (◦◦◦) Fourier transform of the k^3-weighted EXAFS spectra at uranium L_3 edge for organic samples 1 (DEHiBA-uranyl nitrato complexes, $[\overline{Tc}]/[\overline{U}]=0$), 2 and 3 (DEHiBA-uranyl pertechnetate nitrato complexes, $[\overline{Tc}]/[\overline{U}]=0.6$ and 2.4 respectively).

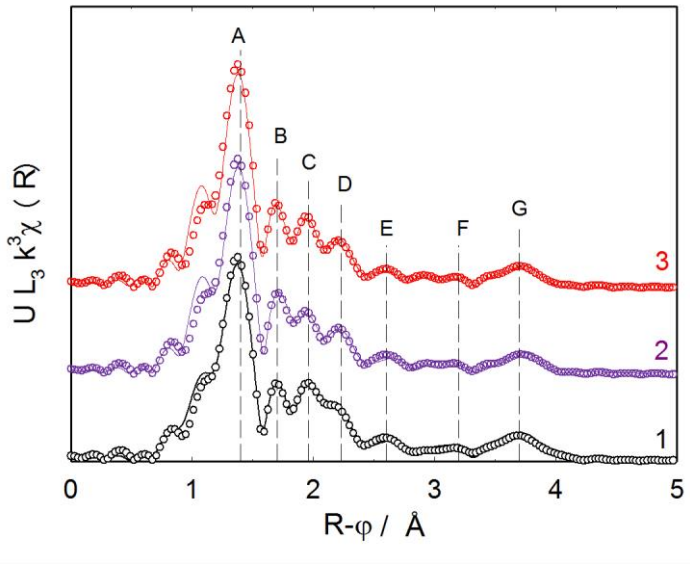

Figure 10. Experimental (—) and fitted (◦◦◦) Fourier transform of the k^3-weighted EXAFS spectra at uranium L_3 edge for organic samples 1 (DEHiBA-uranyl nitrato complexes), 2 and 3 (DEHiBA-uranyl pertechnetate nitrato complexes).

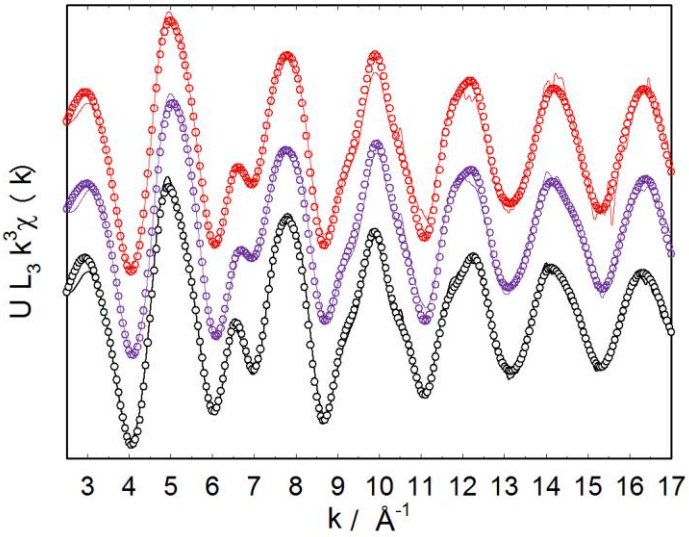

Figure 11. Experimental (—) and fitted (◦◦◦) k^3-weighted EXAFS spectra at uranium L_3 edge for organic samples 1 (DEHiBA-uranyl nitrato complexes), 2 and 3 (DEHiBA-uranyl pertechnetate nitrato complexes).

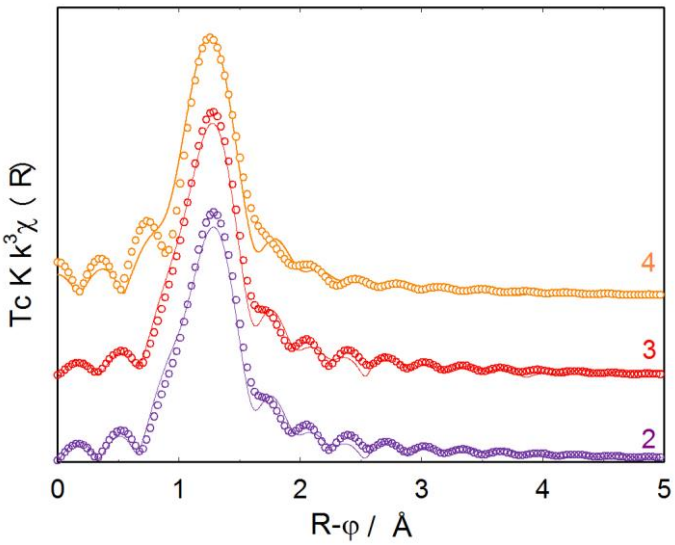

Figure 12. Experimental (—) and fitted (◦◦◦) Fourier transform of the k^3-weighted EXAFS spectra at technetium K edge for organic samples 2, 3 (DEHiBA-uranyl pertechnetate nitrato complexes) and 4 (DEHiBA- pertechnetate complexes).

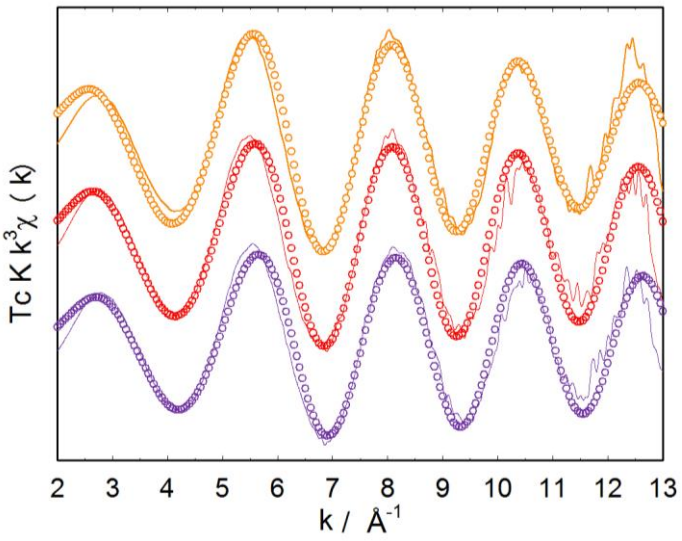

Figure 13. Experimental (—) and fitted (◦◦◦) k^3-weighted EXAFS spectra at technetium K edge for organic samples 2, 3 (DEHiBA-uranyl pertechnetate nitrato complexes) and 4 (DEHiBA-pertechnetate complexes).

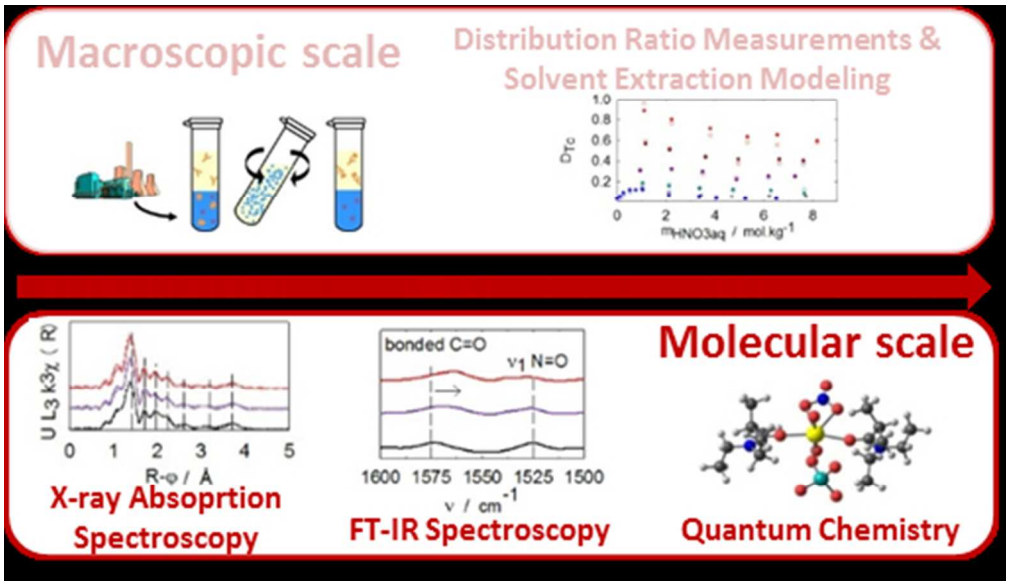

The co-extraction mechanism of technetium(VII) in the presence of uranium(VI) by the N,N-dialkyl amide DEHiBA was elucidated. By combining a macroscopic approach (distribution data acquisition and modeling) with molecular-scale investigations (FT-IR and X-ray absorption analysis supported by theoretical calculations), a new insight into the description of solvent extraction mechanism is provided.
86x49mm (150 x 150 DPI)